Journal of Organometallic Chemistry 694 (2009) 1317–1324

Contents lists available at ScienceDirect

Journal of Organometallic Chemistry

journal homepage: www.elsevier.com/locate/jorganchem

High-efficiency solution processable electrophosphorescent iridium complexes bearing polyphenylphenyl dendron ligands

Chun Huang [a,b], Chang-Gua Zhen [a], Siew Ping Su [a], Zhi-Kuan Chen [a,*], Xiao Liu [c], De-Chun Zou [c], Yan-Rong Shi [c], Kian Ping Loh [b,*]

[a] Institute of Materials Research and Engineering, 3 Research Link, Singapore 117602, Singapore
[b] Department of Chemistry, National University of Singapore, 3 Science Drive, Singapore 117543, Singapore
[c] Department of Chemistry, Peking University, Beijing, 100871, PR China

ARTICLE INFO

Article history:
Received 30 September 2008
Received in revised form 3 December 2008
Accepted 4 December 2008
Available online 16 December 2008

Keywords:
Electrophosphorescent
Polyphenylphenyl dendron
Iridium complexes
OLEDs

ABSTRACT

We report the synthesis and electrophosphorescent behavior of a series of novel iridium complex materials (Complexes **A–F**), which are composed of ligands bearing polyphenylphenyl dendron groups and acetylacetonate. Yellow to saturated red organic light-emitting diodes (OLEDs) based on these newly developed Ir complexes were fabricated through solution process by doping the complex materials into polyvinyl carbazole (PVK)/2-(4-biphenylyl)-5-(4-*tert*-butylphenyl)-1,3,4-oxadiazole (PBD) matrices. The emission wavelengths of the materials could be effectively tuned from 549 nm to 640 nm by changing the conjugation of the ligands either through incorporating additional aromatic segment (e.g. phenyl or fluorenyl group) onto the basic dendron ligand or fusing two of the phenyl rings on the polyphenylphenyl dendron group. High performance devices with the configuration of ITO/poly(3,4-ethylenedioxythiophene):poly(styrenesulfonic acid) (PEDOT:PSS) (50 nm)/PVK:PBD (40%):Ir complex (6%) (70 nm)/2,9-dimethyl-4,7-diphenyl-1,10-phenanthroline (BCP) (12 nm)/Alq_3 (20 nm)/Mg:Ag (150 nm) have been demonstrated. For example, when Complex **B** was used as the emissive layer, maximum current efficiency of 34.0 cd/A and external quantum efficiency of 10.3% have been achieved. When 1,3,5-tris(*N*-phenylbenzimidazol-2-yl) benzene (TPBI) was used as the block layer, the efficiencies can be further improved to 46.3 cd/A and 13.9%, respectively. These solution processed OLED devices demonstrated quite stable EL efficiencies over a large range of current density, which indicated that triplet–triplet annihilation in electrophosphorescence could be effectively suppressed by incorporation of the polyphenylphenyl dendron structure into iridium complexes.

1. Introduction

Electroluminescent materials have attracted significant scientific and industrial attention because of their potential for full-color flat panel displays [1–3]. Recently, heavy metal ion based electrophosphorescent materials, especially iridium-based complex materials, have been intensively investigated as promising candidates for highly efficient OLEDs because: (1) they can harvest both triplet excitons and singlet excitons for light emission in devices due to the strong spin–orbital coupling caused by the heavy metal atoms; (2) their emission can cover the whole visible range through tuning of the ligand structures of the complexes [4–18]. However, it was found that the quantum efficiency of iridium complex-based devices drops quickly due to the triplet–triplet annihilation and concentration quenching of the materials. Obviously, such a drawback will limit the application of iridium complexes for OLEDs. To address this issue, bulky ligands have been used to prevent interactions between Ir-complex molecules and the performance of devices fabricated from these compounds has improved [19,20]. For example, dendrimer type iridium complexes have been demonstrated to prevent the interaction between molecules in solid state effectively and highly efficient OLED devices have been achieved through solution process fabrication with these materials [21–25]. Recently, it has been demonstrated that organic light-emitting materials with fully conjugated polyphenylphenyl dendron groups can also effectively prevent molecular aggregation or π–π stacking and excellent EL efficiencies for both fluorescent small molecular OLEDs and polymeric light-emitting diodes (PLEDs) have been realized [26–29]. The polyphenylphenyl dendron groups could be easily incorporated into the material structure through a simple synthetic procedure. Complex materials with ligands bearing such a polyphenylphenyl dendron structure should also be able to retard the interactions between the molecules and prevent the quenching of electrophosphorescensce in

* Corresponding authors.
E-mail addresses: zk-chen@imre.a-star.edu.sg (Z.-K. Chen), chmlohkp@nus.edu.sg (K.P. Loh).

0022-328X/$ - see front matter © 2008 Elsevier B.V. All rights reserved.
doi:10.1016/j.jorganchem.2008.12.009

devices [30,31]. On the basis of this idea, we recently have developed a series of iridium complex materials (Complexes **A–F**, structures are shown in Fig. 1) bearing polyphenylphenyl dendron groups in the ligands through simple synthesis and purification procedure [32]. It was found that the emission wavelengths of the materials could be effectively tuned by changing the conjugation of the ligands either through incorporating additional aromatic segment onto the basic dendron ligand or fusing two of the phenyl rings on the polyphenylphenyl dendron group. Good performance of OLED devices emitting yellow to saturated red light has been achieved by using these newly developed complex materials as emissive layer through solution process. Although the synthesis of Complex **D** has been reported by Lin et al. [30], no OLED device has been demonstrated yet. Thus, Complex **D** is also included in this report and its OLED performance will be compared with other complexes.

2. Experimental

2.1. Materials synthesis

2.1.1. Synthesis of compound ***1a***

To a solution of 2-bromopyridine (4.74 g, 0.030 mol), CuI (0.14 g, 0.74 mmol), and $Pd(PPh_3)_2Cl_2$ (0.52 g, 0.74 mmol) in 100 ml of diisopropylamine was added (trimethylsilyl)acetylene (3.0 g, 0.030 mol). The mixture was stirred at room temperature overnight under nitrogen atmosphere. After removal of the solvent in vacuo, the residue was distilled under reduced pressure to offer 5.0 g (yield 95%) of pure 2-(trimethylsilyl)ethynyl-pyridine (**1a**). MS: *m/z* 175.2 (27%). ^{1}H NMR (400 MHz, $CDCl_3$) δ (ppm): 8.52 (d, *J* = 4.7 Hz, 1H), 7.57 (d, *J* = 7.7 Hz, 1H), 7.39 (m, 1H), 7.16 (m, 1H), 0.22 (s, 9H).

2.1.2. Synthesis of compound ***1b***

To a solution of 2,5-dibromopyridine (3.56 g, 0.015 mol), CuI (0.07 g, 0.37 mmol), and $Pd(PPh_3)_2Cl_2$ (0.26 g, 0.37 mmol) in 100 ml of diisopropylamine was added (trimethylsilyl)acetylene (1.47 g, 0.015 mol). The mixture was stirred at room temperature overnight under nitrogen atmosphere. After removal of the solvent in vacuo, the residue was purified by flash column to offer 3.45 g (yield 90%) of 2-(trimethylsilyl)ethynyl-5-bromopyridine (**1b**). MS: *m/z* 252.8 (47%), 254.8 (47%). ^{1}H NMR (400 MHz, $CDCl_3$) δ (ppm): 8.640 (s, 1H), 7.801 (d, *J* = 8.0 Hz, 1H), 7.368 (d, *J* = 8.0 Hz, 1H), 0.289 (s, 9H).

2.1.3. Synthesis of compound ***2a (Ligand A)***

To a solution of 2-(trimethylsilyl)ethynyl-pyridine (**1a**) (0.88 g, 5 mmol) in a mixture of THF (10 ml) and methanol (2 ml) was added 1 ml of NaOH (5 N). After the reaction mixture was stirred for 1 h at room temperature, 50 ml of ethyl acetate was added. The mixture was washed with water and brine and dried with anhydrous magnesium sulfate. After the solvent was removed in vacuo, the residue was refluxed with tetraphenylcyclopentadienone (2.0 g, 5.2 mmol) in 50 ml o-xylene overnight. After being cooled down to room temperature, the solvent was removed by flash column and the residue was purified by recrystallization in ethanol 2–3 times to offer 1.95 g of pure 2-(2',3',4',5'-tetraphenyl)phenylpyridine (yield 85%). MS: *m/z* 458.1 (100%). ^{1}H NMR (400 MHz, $CDCl_3$) δ (ppm): 8.06 (d,*J* = 4.0 Hz, 1H), 7.82 (s, 1H), 7.384 (t, 1H), 7.18 (m, 5H), 7.09 (m, 1H), 6.98–6.89 (m, 14H), 6.825 (m, 2H). ^{13}C NMR (100 MHz, $CDCl_3$) δ (ppm): 142.00, 142.03, 141.55, 140.82, 140.54, 140.32, 140.24, 140.12, 139.51, 135.37, 131.87, 131.84, 131.76, 131.57, 130.39, 127.86, 127.47, 127.29, 127.04, 126.60, 126.04, 125.80, 125.62.

2.1.4. Synthesis of compound ***2b***

To a solution of 2-(trimethylsilyl)ethynyl-5-bromopyridine (**1b**) (1.27 g, 5 mmol) in a mixture of THF (10 ml) and methanol (2 ml) was added 1 ml of NaOH (5 N). The reaction mixture was stirred for 1 h at room temperature. Then 50 ml of ethyl acetate was added and the mixture was washed with water, brine and dried with anhydrous magnesium sulfate. After the solvent was removed, the residue was refluxed with tetraphenylcyclopentadienone (2.0 g, 5.2 mmol) in 50 ml o-xylene overnight. After being cooled down to room temperature, the solvent was removed by flash column and the residue was purified by recrystallization in ethanol 2–3 times to offer 2.17 g of pure 2-(2',3',4',5'-tetraphenyl)phenyl-5-bromopyridine (**2b**) (yield 81%). MS: *m/z* 537.9 (100%), 535.8 (100%). ^{1}H NMR (400 MHz, $CDCl_3$) δ (ppm): 8.659 (d, *J* = 2 Hz, 1H), 7.803 (s, 1H), 7.490 (d, 1H), 7.165 (s, 5H), 7.017-6.769 (m, 16H).

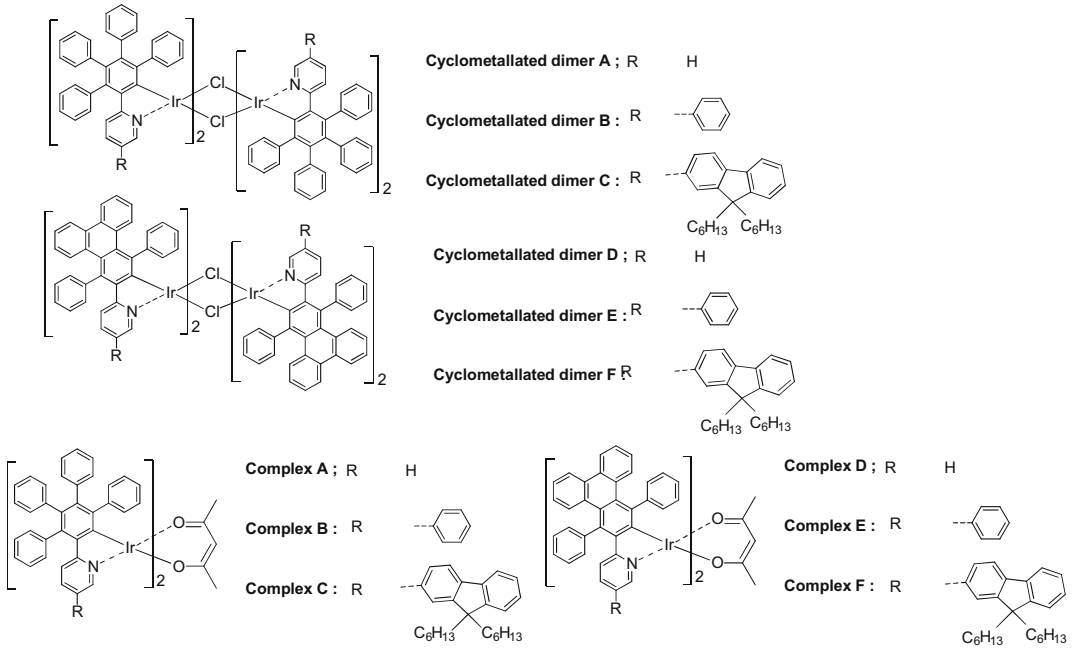

Fig. 1. Chemical structures of Complexes **A–F**.

*2.1.5. Synthesis of Ligand **B***

In an argon flushed two-neck round-bottom flask, a mixture of 1.60 g (3.0 mmol) of compound **2b**, 0.5 g (4 mmol) of phenyl boronic acid, 36 mg (1 mol%) of tetrakis(triphenylphosphine)palladium(0), 15 ml of 2 M sodium carbonate and 30 ml of toluene was added and heated at reflux for 2 h. After being cooled down to room temperature, the reaction mixture was extracted with ethyl acetate and the organic phase was washed with water and brine and dried over magnesium sulfate. The solvent was then removed in vacuo and the residue was purified by flash column eluted with hexane/CH_2Cl_2 (3:1) followed by recrystallization in ethanol to provide 1.48 g of Ligand **B** (yield 92%). MS: *m/z* 534.2 (100%). ^{1}H NMR (400 MHz, $CDCl_3$) δ (ppm): 8.68 (s, 1H), 7.91 (s, 1H), 7.60 (d, 3H), 7.50 (d, 2H), 7.42 (m, 1H), 7.20 (t, 5H), 7.00–6.83 (m, 16H). ^{13}C NMR (100 MHz, $CDCl_3$) δ (ppm): 158.48, 147.89, 142.19, 142.03, 141.64, 140.93, 140.55, 140.33, 140.29, 139.68, 139.57, 138.02, 134.22, 133.74, 131.90, 131.84, 131.79, 131.69, 130.41, 129.93, 129.42, 128.35, 127.89, 127.62, 127.38, 127.32, 127.07, 126.64, 126.34, 126.07, 125.83, 125.51.

*2.1.6. Synthesis of Ligand **C***

The procedure used is the same as that for preparation of Ligand **B**. 1.60 g (3.0 mmol) of **2b**, 1.51 g (4 mmol) of 2-(9,9-dihexyl)-fluorenyl boronic acid, 36 mg (1 mol%) of tetrakis(triphenylphosphine)palladium(0), 15 ml of 2 M sodium carbonate and 30 ml of toluene were added in a round-bottom flask and heated at reflux for 2 h. After normal work-up, the crude product was purified by flash column eluted with hexane/CH_2Cl_2 (4:1) followed by recrystallization in ethanol to provide 1.99 g of Ligand **C** (yield 84%). MS: *m/z* 791.4 (100%). ^{1}H NMR (400 MHz, $CDCl_3$) δ (ppm): 8.93 (s, 1H), 7.98 (s, 1H), 7.78 (m, 2H), 7.66 (d, 1H), 7.57 (m, 2H), 7.38 (m, 3H), 7.20 (t, 5H), 7.03–6.96 (m, 9H), 6.90 (m, 5H), 6.83 (m, 2H), 2.03 (t, 4H), 1.13–1.06 (m, 12H), 0.79–0.67 (m, 10H). ^{13}C NMR (100 MHz, $CDCl_3$) δ (ppm): 158.50, 152.08, 151.36, 148.02, 142.24, 142.03, 141.64, 141.52, 140.90, 140.56, 140.37, 140.34, 139.70, 139.50, 136.38, 134.73, 133.67, 131.89, 131.84, 130.41, 127.89, 127.71, 127.64, 127.31, 127.24, 127.06, 126.62, 126.33, 126.21, 126.06, 125.81, 125.50, 123.32, 121.56, 120.55, 120.26, 55.62, 40.78, 31.86, 30.07, 24.14, 22.96, 14.38.

*2.1.7. Synthesis of compound **3a** (Ligand **D**)*

The procedure used is the same as that for preparation of compound **2a**. 0.88 g (5 mmol) of 2-(trimethylsilyl)ethynyl-pyridine (**1a**) was converted to 2-ethynyl-pyridine in a mixture of THF (10 ml) and methanol (2 ml) containing 1 ml of NaOH (5 N). The obtained crude product of 2-ethynyl-pyridine was refluxed with phencyclone (2.0 g, 5.2 mmol) in 50 ml o-xylene overnight. After being cooled down to room temperature, the solvent was removed by flash column and the residue was purified by recrystallization in ethanol 2–3 times to offer 1.95 g (yield 85%) of Ligand **D**. MS: *m/z* 456.1 (100%). ^{1}H NMR (400 MHz, $CDCl_3$) δ (ppm): 8.68 (d, J = 4.0 Hz, 1H), 8.48 (d, J = 8.0 Hz, 2H), 7.91 (s, 1H), 7.81 (d, J = 8.0 Hz, 1H), 7.56–7.21 (m, 16H), 6.95 (m, 1H), 6.71 (m, 1H). ^{13}C NMR (100 MHz, $CDCl_3$) δ (ppm): 159.90, 149.70, 144.76, 142.37, 139.41, 138.97, 136.95, 135.24, 132.34, 132.26, 132.08, 132.04, 131.86, 131.38, 131.08, 130.56, 130.27, 130.09, 129.37, 129.02, 127.54, 127.30, 127.22, 126.85, 126.00, 125.96, 125.69, 123.63, 123.60, 121.48.

*2.1.8. Synthesis of compound **3b***

To a solution of 2-(trimethylsilyl)ethynyl-5-bromopyridine (**1b**) (1.27 g, 5 mmol) in a mixture of THF (10 ml) and methanol (2 ml) was added 1 ml of NaOH (5 N). The reaction mixture was stirred for 1 h at room temperature. 50 ml of ethyl acetate was added and washed with water, brine and then dried with anhydrous magnesium sulfate. After the solvent was removed, the residue was refluxed with phencyclone (2.0 g, 5.2 mmol) in 50 ml o-xylene overnight. After being cooled down to room temperature, the solvent was removed by flash column and the residue was purified by recrystallization in ethanol 2–3 times to offer 2.00 g (about yield 75%) of **3b** with small amount of impurity. Compound **3b** was used for next step synthesis without further purification.

*2.1.9. Synthesis of Ligand **E***

The procedure used is the same as that for preparation of Ligand **B**. 1.60 g (3.0 mmol) of **3b**, 0.5 g (4 mmol) of phenyl boronic acid, 36 mg (1 mol%) of tetrakis(triphenylphosphine)palladium(0), 15 ml of 2 M sodium carbonate and 30 ml of toluene were added in a round-bottom flask and heated at reflux for 2 h. After normal work-up, the crude product was purified by flash column eluted with hexane/CH_2Cl_2 (3:1) followed by recrystallization in ethanol to provide 1.43 g of Ligand **E** (yield 92%). MS: *m/z* 532.2 (100%). ^{1}H NMR (400 MHz, $CDCl_3$) δ (ppm): 8.93 (s, 1H), 8.48, (d, J = 8.0 Hz, 2H), 7.98 (s, 1H), 7.82 (d, J = 8.0 Hz, 1H), 7.63 (d, 3H), 7.58–7.38 (m, 11H) 7.28–7.24 (m, 5H), 7.16 (t, 1H), 7.06 (t, 1H), 6.72 (d, J = 8.0 Hz, 1H). ^{13}C NMR (100 MHz, $CDCl_3$) δ (ppm): 158.48, 147.89, 142.19, 142.03, 141.64, 140.93, 140.55, 140.33, 140.29, 139.68, 139.57, 138.02, 134.22, 133.74, 131.90, 131.84, 131.79, 131.69, 130.41, 129.93, 129.42, 128.35, 127.89, 127.62, 127.38, 127.32, 127.07, 126.64, 126.34, 126.07, 125.83, 125.51.

*2.1.10. Synthesis of Ligand **F***

The procedure used is the same as that for preparation of Ligand **B**. 1.60 g (3.0 mmol) of **3b**, 1.51 g (4 mmol) of 2-(9,9-dihexyl)-fluorenyl boronic acid, 36 mg (1 mol%) of tetrakis(triphenylphosphine)palladium(0), 15 ml of 2 M sodium carbonate and 30 ml of toluene were added in a round-bottom flask and heated at reflux for 2 h. After normal work-up, the crude product was purified by flash column eluted with hexane/CH_2Cl_2 (4:1) followed by recrystallization in ethanol to provide 2.0 g Ligand **F** (yield 85%). MS: *m/z* 789.1 (100%). ^{1}H NMR (400 MHz, $CDCl_3$) δ (ppm): 8.99 (s, 1H), 8.48 (d, J = 8.0 Hz, 2H), 8.00 (s, 1H), 7.81 (d, J = 8.0 Hz, 2H), 7.76 (d, J = 8.0 Hz, 1H), 7.60 (d, J = 8.0 Hz, 1H), 7.56–7.36 (m, 13H), 7.30 (m, 5H), 7.14 (t, 1H), 7.07 (t, 1H), 6.74 (d,, J = 8.0 Hz, 1H), 2.04 (t, 4H), 1.14 (12H), 0.77 (10H). ^{13}C NMR (100 MHz, $CDCl_3$) δ (ppm): 158.50, 152.13, 151.38, 148.21, 144.75, 142.42, 141.57, 140.85, 138.99, 136.98, 136.69, 134.70, 133.52, 132.52, 132.37, 132.15, 132.11, 131.88, 131.42, 131.09, 130.56, 130.25, 130.10, 129.38, 129.18, 127.73, 127.56, 127.42, 127.26, 126.86, 126.24, 126.02, 125.79, 125.69, 123.65, 123.60, 123.34, 121.60, 123.34, 121.60, 120.58, 120.28, 55.63, 40.78, 31.87, 30.09, 24.16, 22.97, 14.40.

*2.2. General procedure for synthesis of Cyclometallated dimmer **A–F***

In a mixture solvent of 2-ethoxyethanol and water (3:1) (30 ml), 0.2 g (0.57 mmol) of $IrCl_3{\cdot}3H_2O$ and 1.45 mmol of ligand compound were added. The reaction mixture was refluxed overnight and precipitate was formed. The precipitate was filtered when the reaction was cooled down to room temperature and washed with water and ethanol successively. The cyclometallated dimer products were obtained after drying in vacuo. Cyclometallated dimer **A**, yield 78%; Cyclometallated dimer **B**, yield 68%; Cyclometallated dimer **C**, yield 71%; Cyclometallated dimer **D**, yield 68%; Cyclometallated dimer **E**, yield 71%; Cyclometallated dimer **F**, yield 75%.

*2.3. General procedure for synthesis of Complexes **A–F***

In an argon flushed two-neck 50 ml round-bottom flask, a mixture of 0.1 mmol of cyclometallated dimer product, 0.1 g (1 mmol) of 2,4-pentanedione in 1 ml ethanol, 0.5 ml tetramethylammoniumhydroxide (25% in methanol), 5 ml ethanol, and

30 ml of CH_2Cl_2 was added and heated at reflux for 5 h. After cooled down to room temperature, the reaction mixture was washed with brine and dried over magnesium sulfate. The solvent was then removed in vacuo and the residue was refluxed in heptane later filtered when it is still hot to provide the complex material with a yield of 70–80%.

2.3.1. Complex **A**

Yield: 79%. ^{1}H NMR (400 MHz, $CDCl_3$) δ (ppm): 8.562– 8.551 (d, J = 4.4 Hz, 2H), 7.380–7.359 (d, J = 8.4 Hz, 2H), 7.320–7.303 (d, J = 6.8 Hz, 2H), 7.236–7.120 (m, 8H), 7.101–7.013 (m, 6H), 6.979–6.966 (m, 2H), 6.938–6.870 (m, 4H), 6.870–6.787 (m, 4H), 6.777–6.758 (d, J = 7.6 Hz, 2H), 6.738–6.708 (m, 2H), 6.688–6.669 (d, J = 7.6 Hz, 2H), 6.619–6.602 (d, J = 6.8 Hz, 2H), 6.531–6.516 (d, J = 6.0 Hz, 2H), 6.467–6.446 (d, J = 8.4 Hz, 2H), 6.205–6.168 (t, J = 7.4 Hz, 2H), 6.062–6.043 (d, J = 7.6 Hz, 2H), 5.981–5.964 (d, J = 6.8 Hz, 2H), 5.208 (s, 1H), 2.048 (s, 6). MS (MALDI-TOF): *m/z Calc.* for $C_{75}H_{55}IrN_2O_2$ 1208.389; found 1208.365. Element Anal.: Calc. for $C_{75}H_{55}IrN_2O_2$: C, 74.54; H, 4.59; N, 2.32; found: C, 74.13; H, 4.38; N, 1.99%.

2.3.2. Complex **B**

Yield: 71%. ^{1}H NMR (400 MHz, $CDCl_3$) δ (ppm): 8.198–8.193 (d, J = 2.0 Hz, 2H), 7.384–7.353 (t, J = 6.4 Hz, 8H), 7.350–7.297 (m, 4H), 7.26–7.213 (m, 2H), 7.146–7.112 (m, 4H), 7.030–7.018 (m, 2H), 7.005–6.977 (dd, J = 9.0 Hz, 2.4 Hz, 2H), 6.909–6.890 (d, J = 7.6 Hz, 2H), 6.86–6.81 (m, 4H), 6.81–6.74 (m, 8H), 6.724–6.704 (m, 2H), 6.66–6.61 (m, 4H), 6.605–6.522 (tt, J = 7.2 Hz, 4H), 6.484–6.465 (d, J = 7.6 Hz, 2H), 6.379–6.342 (t, 7.4 Hz, 2H), 6.164–6.128 (t, 7.6 Hz, 2H), 5.900–5.877 (d, J = 9.2 Hz, 2H), 5.056 (s, 1H), 1.791 (s, 6H). MS (MALDI-TOF): *m/z Calc.* for $C_{87}H_{63}IrN_2O_2$ 1360.452; found 1360.482. Element Anal.: Calc. for $C_{87}H_{63}IrN_2O_2$: C, 76.80; H, 4.67; N, 2.06; found: C, 76.99; H, 4.63; N, 2.02%.

2.3.3. Complex **C**

Yield: 73%. ^{1}H NMR (400 MHz, $CDCl_3$) δ (ppm): 8.087–8.084 (d, J = 1.2 Hz, 2H), 7.707–7.688 (d, J = 7.6 Hz, 4H), 7.37–7.30 (m, 6H), 7.291–7.253 (t, J = 7.2 Hz, 4H), 7.25–7.17 (m, 4H), 7.17–7.09 (m, 8H), 7.030–7.010 (d, J = 8.0 Hz, 2H), 6.89–6.81 (m, 6H), 6.800–6.782 (m, 4H), 6.759–6.739 (d, J = 8.0 Hz, 2H), 6.73–6.69 (m, 2H), 6.69–6.61 (m, 6H), 6.492–6.474 (d, J = 7.2 Hz, 2H), 6.46–6.39 (m, 2H), 6.345–6.326 (m, 4H), 6.049–6.027 (d, J = 8.8 Hz, 2H), 5.325 (s, 1H), 1.998–1.945 (m, 8H), 1.922 (s, 6H), 1.124–1.050 (m, 24H), 0.755–0.724 (t, J = 6.2 Hz, 12H), 0.686–0.547 (m, 8H). MS (MALDI-TOF): *m/z Calc.* for $C_{125}H_{119}IrN_2O_2$ 1872.890; found 1872.943. Element Anal.: Calc. for $C_{125}H_{119}IrN_2O_2$: C, 80.13; H, 6.40; N, 1.50; found: C, 80.33; H, 6.21; N, 1.65%.

2.3.4. Complex **D**

Yield: 66%. ^{1}H NMR (400 MHz, $CDCl_3$) δ (ppm): 8.580–8.560 (d, J = 8.0 Hz, 2H), 8.362–8.298 (m, 6H), 8.087–8.069 (d, J = 7.2 Hz, 2H), 7.750–7.735 (m, 4H), 7.465–7.398 (m, 4H), 7.382–7.261 (m, 8H), 7.013–6.973 (t, J = 8.0 Hz, 4H), 6.865–6.794 (m, 4H), 6.538–6.509 (m, 4H), 6.449–6.399 (m, 4H), 5.822–5.801 (d, J = 8.4 Hz, 2H), 5.001 (s, 1H), 2.104 (s, 6H). MS (MALDI-TOF): *m/z Calc.* for $C_{75}H_{51}IrN_2O_2$ 1204.358; found 1204.440. Element Anal.: Calc. for $C_{75}H_{51}IrN_2O_2$: C, 74.79; H, 4.27; N, 2.33; found: C, 74.91; H, 4.25; N, 2.24%.

2.3.5. Complex **E**

^{1}H NMR (400 MHz, $CDCl_3$) δ (ppm): 8.357–8.336 (d, J = 8.4 Hz, 2H), 8.305–8.284 (d, J = 8.4 Hz, 2H), 8.136–8.117 (d, J = 7.6 Hz, 2H), 7.839–7.770 (m, 4H), 7.468–7.394 (m, 10H), 7.338–7.191 (m, 16H), 7.030–6.992 (t, J = 7.6 Hz, 2H), 6.966–6.939 (dd, J = 8.8 Hz, J = 1.0 Hz, 2H), 6.856–6.817 (t, J = 7.8 Hz, 2H), 6.525–6.489 (t, J = 7.2 Hz, 2H), 6.395–6.310 (m, 6H), 5.873–5.851 (d, J = 8.8 Hz, 2H), 5.025 (s, 1H), 1.847 (s, 6H). Yield: 81%. MS (MALDI-TOF): *m/z Calc.* for $C_{87}H_{59}IrN_2O_2$ 1356.421; found 1356.526. Element Anal.: Calc. for $C_{87}H_{59}IrN_2O_2$: C, 77.02; H, 4.38; N, 2.06; found: C, 77.28; H, 4.72; N, 2.19%.

2.3.6. Complex **F**

Yield: 70%. ^{1}H NMR (400 MHz, $CDCl_3$) δ (ppm): 8.586–8.567 (d, J = 7.6 Hz, 2H), 8.364–8.318 (t, J = 9.2 Hz, 6H), 7.952–7.949 (d, J = 1.2 Hz, 2H), 7.758–7.728 (m, 4H), 7.593–7.574 (d, J = 7.6 Hz, 2H), 7.473–7.458 (m, 2H), 7.432–7.335 (m, 8H), 7.319–7.226 (m, 6H), 7.215–7.088 (m, 6H), 7.046–7.025 (d, J = 8.4 Hz, 2H), 6.878–6.860 (d, J = 7.2 Hz, 2H), 6.842–6.803 (t, J = 7.8 Hz, 2H), 6.758–6.721 (t, J = 7.4 Hz, 2H), 6.694–6.655 (t, J = 7.8 Hz, 2H), 6.616–6.581 (t, J = 7.0 Hz, 2H), 6.527–6.446 (m, 4H), 5.864–5.842 (d, J = 8.8 Hz, 2H), 5.097 (s, 1H), 2.182 (s, 6H), 2.135–1.983 (m, 8H), 1.226–1.021 (m, 24H), 0.792–0.759 (t, J = 6.6 Hz, 12H), 0.744–0.610 (m, 8H). MS (MALDI-TOF): *m/z Calc.* for $C_{125}H_{115}IrN_2O_2$ 1868.859; found 1868.965. Element Anal.: Calc. for $C_{125}H_{115}IrN_2O_2$: C, 80.31; H, 6.20; N, 1.50; found: C, 80.14; H, 6.04; N, 1.52%.

2.2. Spectroscopy and electrochemical measurement

Nuclear magnetic resonance (NMR) spectra were collected on a Bruker ACF 400 spectrometer using chloroform-*d* as a solvent and tetramethylsilane (TMS) as an internal standard. Ultraviolet–Visible (UV–Vis) spectra of the materials in $CHCl_3$ at room temperature with concentration of $\sim 1 \times 10^{-5}$ M were obtained using a Shimadzu UV 3101PC UV–Vis-NIR spectrophotometer with a xenon lamp in the scan rate of 300 nm/min. Photoluminescence (PL) spectra of the materials in $CHCl_3$ at room temperature with concentration of $\sim 3 \times 10^{-6}$ M were obtained with a Perkin Elmer LS 50B luminescence spectrometer with the excitation at λ_{max} of the UV–Vis absorption spectra. Cyclic voltammetry (CV) experiments were conducted on an AUTOLAB (model PGSTAT30) workstation under argon atmosphere. All potentials were measured in a three-electrode cell with 0.10 M tetrabutylammonium perfluorate phosphate (Bu_4NPF_6) in anhydrous acetonitrile as the electrolyte, using a Ag/AgCl (3 M KCl) electrode as the reference electrode (−0.040 V versus SCE), a platinum wire as the counter electrode and a platinum disc as the working electrode. All experimental values were corrected with respect to SCE. The HOMOs of the compounds are estimated from onset potentials for oxidation of the p-doping processes using the equation $E_{HOMO} = -[4.4 + E^{ox}_{onset}]$ eV [33,34] and the LUMOs are thus estimated incorporating the HOMOs from electrochemical measurements and the HOMO–LUMO gap estimated from the UV spectra edge from equation of $E_{gap} = -[E_{HOMO} - E_{LUMO}]$. The onset potentials were determined from the intersection of the two tangents drawn at the rising current and baseline charging current of the CV curves.

2.3. LED device fabrication

A first layer of poly(3,4-ethylenedioxythiophene) doped with poly(styrenesulfonic acid) (PEDOT:PSS) was spin-coated on a pretreated glass substrate with patterned ITO to form a hole injection layer with a thickness of about 50 nm. After being dried in oven at 120 °C for 15 min, a solution containing 4 ml chlorobenzene, 27 mg PVK, 20 mg PBD, and 3.0 mg iridium complex material was spin-coated onto the first layer to form the emitting layer with a thickness of about 70 nm. On the emissive layer, 12 nm of BCP, 20 nm of Alq_3, 150 nm of Mg:Ag, and 10 nm of Ag were thermally deposited sequentially under vacuum of 3×10^{-4} Pa. The organic electroluminescent devices obtained were examined in a glove box. EL spectra were recorded with an Ocean Optics USB2000 Miniature Fiber Optic Spectrometer.

3. Results and discussion

The ligand compounds and the resulting complex materials Complex **A–F** were achieved with high yields through simple synthesis and purification procedure following the synthetic routes outlined in Scheme 1. Only recrystallization or flash column chromatography is needed to obtain the target compounds with satisfactory purity. Ethynyl groups were firstly incorporated through palladium-catalyzed Sonogashira coupling reaction onto pyridyl ring with high selectivity and yield because of the high activity of the 2-bromo position on pyridyl ring. Polyphenylphenyl dendron groups were then introduced through the Diels-Alder cycloaddition reaction of 2-ethynylpyridine or 2-ethynyl-5-bromo-pyridine. Another aromatic segment was incorporated to form Ligand **B**, **C**, **E**, and **F** through the Suzuki coupling reaction with high yields. Precipitates of the cyclometallated iridium dimers were formed after the ligand compounds were refluxed with iridium trichloride in 2-ethoxyethanol/H_2O overnight. The dimeric compounds were then refluxed in methylene chloride in the presence of 2,4-pentanedione, $N(Me)_4OH$ and a small amount of ethanol to achieve the final complexes with yields ranging from 65% to 80%. Column purification is also not necessary in the final step. Pure Complex **A–F** can be achieved by treating the crude products in refluxed heptane and filtering out the solid product.

The UV–Vis and photoluminescence (PL) spectra of the complexes are shown in Fig. 2. The UV–Vis absorption over 400 nm is assigned to metal-to-ligand charge transfer (MLCT) transition [6,19]. The higher energy absorptions, which are more intensive, are assigned to the π–π^* ligand absorption. Obviously, the energy band gaps can be tuned by changing the conjugation of the ligands. Increasing the conjugation length by incorporating additional aromatic segments onto the pyridyl rings of the ligands, or fusing two of the phenyl rings in the dendron groups, cause significantly bathochromic shift of both the ligand absorption band and metal-to-ligand charge transfer (MLCT) transition band. For example, the absorption of the MLCT band of Complex **A** is peaked at 405 nm; whilst the maxima MLCT transition of Complexes **B**, **C**, **D**, **E**, **F** are red shifted to 443 nm, 455 nm, 476 nm, 495 nm, and 508 nm, respectively. The PL spectra of the complexes follow the same trend. It was found that λ_{max} of the PL spectra of the complex materials in chloroform could be tuned from 528 nm to 643 nm.

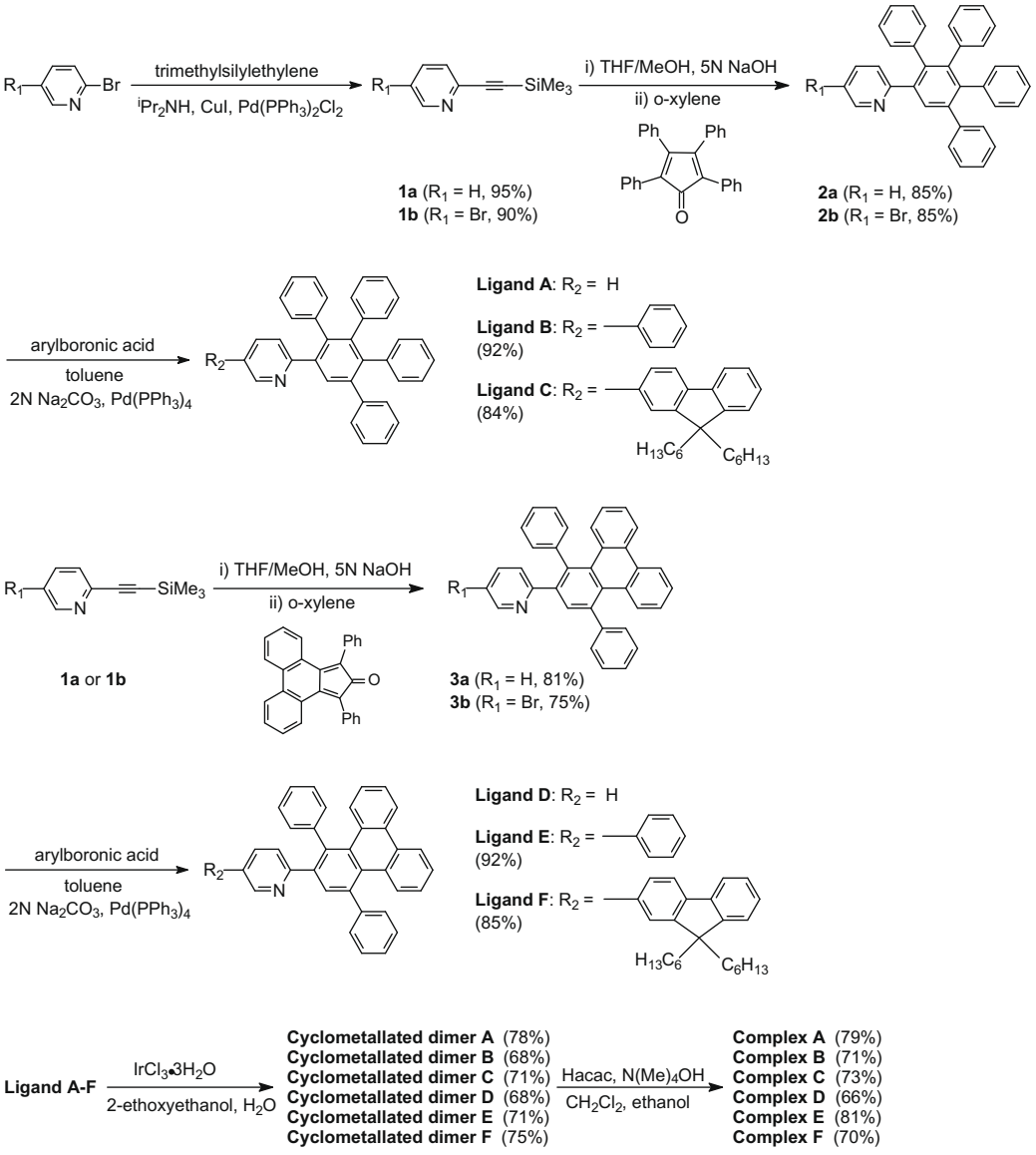

Scheme 1. The synthetic procedure for Complexes **A–F**.

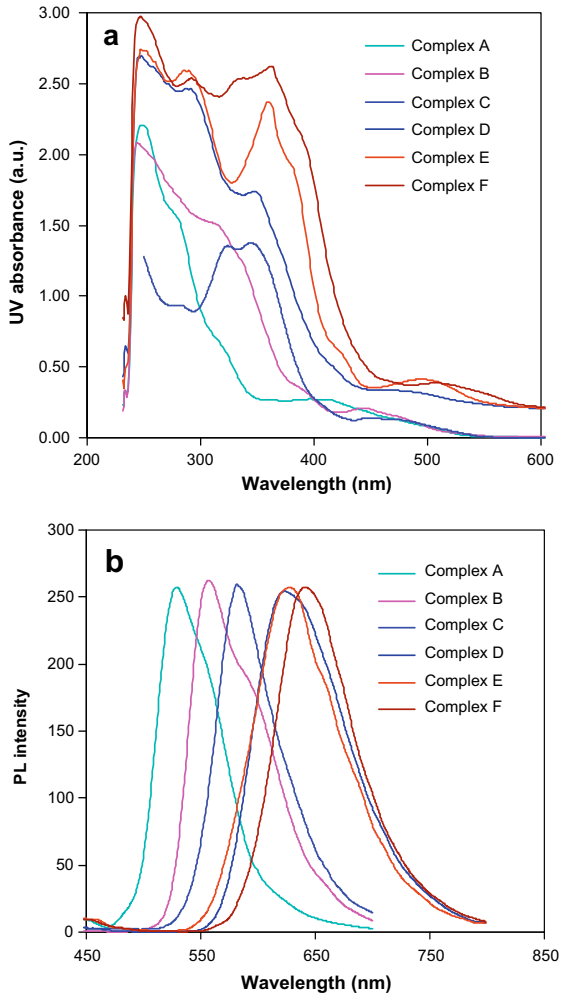

Fig. 2. UV (a) and PL (b) spectra of Complexes **A–F** in chloroform solutions.

Tuning the conjugation length of the ligands will affect not only the bandgaps of the complexes but also their energy levels. The cyclic voltammetric measurements of the complexes in acetonitrile with 0.10 M of tetrabutylammonium hexafluorophosphate (Bu_4NPF_6) as the electrolyte under argon atmosphere indicated that the HOMO of the complexes could be raised by about 0.3–0.4 eV through increasing the conjugation length of the ligands. The LUMOs can be elevated by about 0.2 eV, which are deduced from the HOMO energy levels and the bandgaps obtained from the UV absorption edges of the complexes. The CV measurement results of the complexes are summarized in Table 1 and also drawn in Fig. 5. It should be mentioned that none of the complexes showed reversible oxidation in the cyclic voltammetry measurement and no $E_{1/2}$ values were available for these materials. The PL quantum yields of the iridium complexes measured in chloroform solutions using $(ppy)_2Ir(acac)$ as standard are 2.3%, 52%, 50%, 4.4%, 11%, and 12% for Complexes **A–F**, respectively [6,11]. It is interesting to note that incorporation of an additional aromatic segment on the 5-position of the pyridyl ring can largely increase the PL quantum yields. For example, the PL quantum yields of Complexes **B** and **C** are over 50%, while that of Complex **A** is only 2.3%. The same phenomena were observed on Complex **D** to Complex **F**. Lin et al. have reported that Complex **D** showed low PL efficiency and they explained that the possible reason for the low PL efficiency might be attributed to the intramolecular π–π interaction between the pyridyl ring in one ligand and one of the dangling phenyl ring in the other in the complex, which was supported by the single crystal X-ray diffraction study [30]. This explanation may also be applied in Complex **A**. However, it will be a different case for Complexes **B, C, E,** and **F**. In the later 4 complexes, the incorporation of additional phenyl or fluorenyl group on pyridyl ring at 5-position may twist the pyridyl ring and thus suppress the intramolecular π-π interaction between the pyridyl from occurring. All the UV and PL data of the complexes are also summarized in Table 1.

Table 2
Devices performance data.

Materials	Turn-on voltage (V)	L_{max} (V) (cd/m^2)	η_{cur} (max) (cd/A)	η_{ext} (max) (%)	EL λ_{max} (nm)	CIE (x, y)
Complex A	8.7	5701 (20 V)	4.31	1.23	549	(0.417, 0.575)
Complex B	5.2	50867 (20 V)	34.0	10.3	559	(0.474, 0.520)
Complex C	4.5	30543 (18 V)	30.9	10.9	582	(0.530, 0.467)
Complex D	8.5	3176 (20 V)	2.67	2.12	632	(0.635, 0.365)
Complex E	6.2	6138 (19 V)	5.12	5.12	638	(0.652, 0.343)
Complex F	6.5	5697 (19 V)	4.81	5.60	640	(0.668, 0.330)

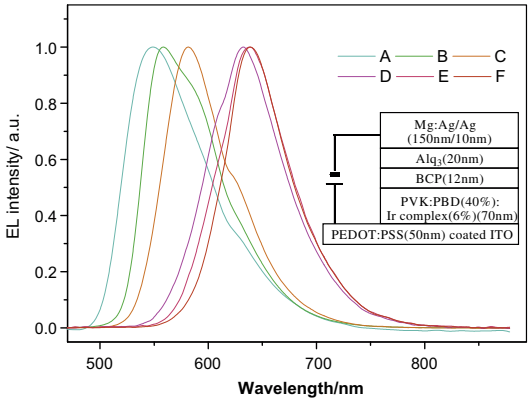

Fig. 3. EL spectra of Complexes **A–F**. Insert shows the OLED device configuration.

Table 1
Physical properties of Complexes **A–F**.

Materials	UV λ_{peak} (MLCT) in $CHCl_3$ (nm)	HOMO–LUMO gaps for the complexes (eV)	PL λ_{max} in $CHCl_3$ (nm)	η_{PL} in $CHCl_3$ (%)	p-Doping (V)		Energy levels (eV)	
					E_{onset}	E_a	HOMO	LUMO
Complex **A**	405	2.27	528	2.3	1.70	2.26	−6.10	−3.83
Complex **B**	443	2.22	557	52	1.47	2.11	−5.87	−3.65
Complex **C**	455	2.18	581	50	1.45	–	−5.85	−3.67
Complex **D**	476	2.12	622	4.4	1.33	1.44/1.86	−5.73	−3.61
Complex **E**	495	2.08	627	11	1.28	1.46/1.88	−5.68	−3.60
Complex **F**	508	2.04	643	12	1.33	1.47/1.86	−5.73	−3.69

In order to understand the electroluminescent properties of Complexes **A–F**, multi-layer OLED devices based on these materials were fabricated and characterized with the configuration of ITO/PEDOT: PSS (50 nm)/PVK:PBD (40%):Ir complex (6%) (70 nm)/BCP (12 nm)/Alq_3 (20 nm)/Mg:Ag (150 nm:10 nm) through solution process. PVK was used as the host material for the device fabrication because its emission spectrum overlaps with the absorption spectra of Complexes **A–F**. BCP (2,9-dimethyl-4,7-diphenyl-1,10-phenanthroline) was used for hole and exciton blocker and PBD (2-*tert*-butylphenyl-5-biphenyl-1,3,4-oxadiazole) was doped to the emission layer to enhance the electron injection and transport ability [7,8]. The key device performance data were summarized in Table 2 and the EL spectra, *I–V–L* curves, and efficiency-current density curves are illustrated in Figs. 3 and 4, respectively.

High performance OLED devices have been demonstrated with these complex materials. According to the EL spectra and CIE coordinates of the devices, the emission light of the complexes could be well tuned by changing the conjugation of the ligands. The turn-on voltages of the devices are in the range of 4.5 and 8.7 V for the six complexes, which are very common for PVK hosted Ir complex-based OLED devices [6,7]. The maximum emission wavelengths of the EL spectra of the devices are from 549 nm to 640 nm. The maximum brightness of the devices are of 5701 cd/m^2 (20 V), 50867 cd/m^2 (20 V), 30543 cd/m^2 (18 V), 3176 cd/m^2 (20 V), 6138 cd/m^2 (19 V), and 5697 cd/m^2 (19 V) for Complexes **A–F** respectively. The maximum EL efficiencies for Complexes **A–F** are 4.31 cd/A (1.23%), 34.0 cd/A (10.3%), 30.9 cd/A (10.9%), 2.67 cd/A (2.12%), 5.12 cd/A (5.12%), 4.81 cd/A (5.60%), respectively. The EL efficiencies of Complexes **B** and **C** are the highest among those PVK based phosphorescent OLED devices [6,7,20], while the EL efficiencies of 5 cd/A (>5%) for saturated red emission materials of Complexes **E** and **F** are also comparable to most of the reference reported results for solution processed devices [9,22]. From the device energy level diagram in Fig. 5, we can find that it is difficult for holes to be injected from PVK (−5.5 eV) [35] to Complexes **A–F** due to their unmatched HOMO energy levels. However, the LUMO energy levels (−3.6 to −3.8 eV) of the complexes are about 1 eV lower than that of PBD (−2.6 eV) [36]. Therefore, electrons could be readily trapped by the complex materials then holes may subsequently hop onto the negative charged phosphorescent molecules to form singlet/triplet excitons [6–8,37,38]. The much lower EL efficiencies of Complexes **A** and **D** than the others may be mainly due to their lower PL efficiencies, which is in good agreement with the reported results by Lin et al. [30]. It is worth mentioning that the high EL efficiencies of the four complexes are stably sustained over a large range of current density, which could be ascribed to the efficacy of polyphenylphenyl dendron groups in the complexes to suppress the triplet–triplet annihilation. The slightly high turn-on voltage of the devices is very common for PVK hosted Ir complexes based OLED devices [6,7].

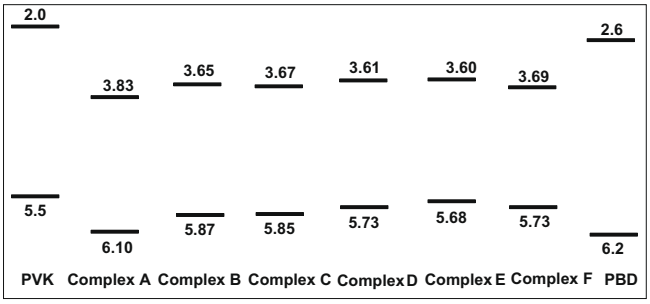

Fig. 5. Energy levels of the complex materials.

In order to further improve device performance, two devices using 1,3,5-tris(*N*-phenylbenzimidazol-2-yl) benzene (TPBI) as the block layer and PVK:PBD:Complex **B**, PVK:PBD:Complex **C** as the emissive zone have been fabricated. The *I–V–L* curves of the two devices are shown in Fig. 6. Both current efficiency and external quantum efficiency for the two devices have been largely

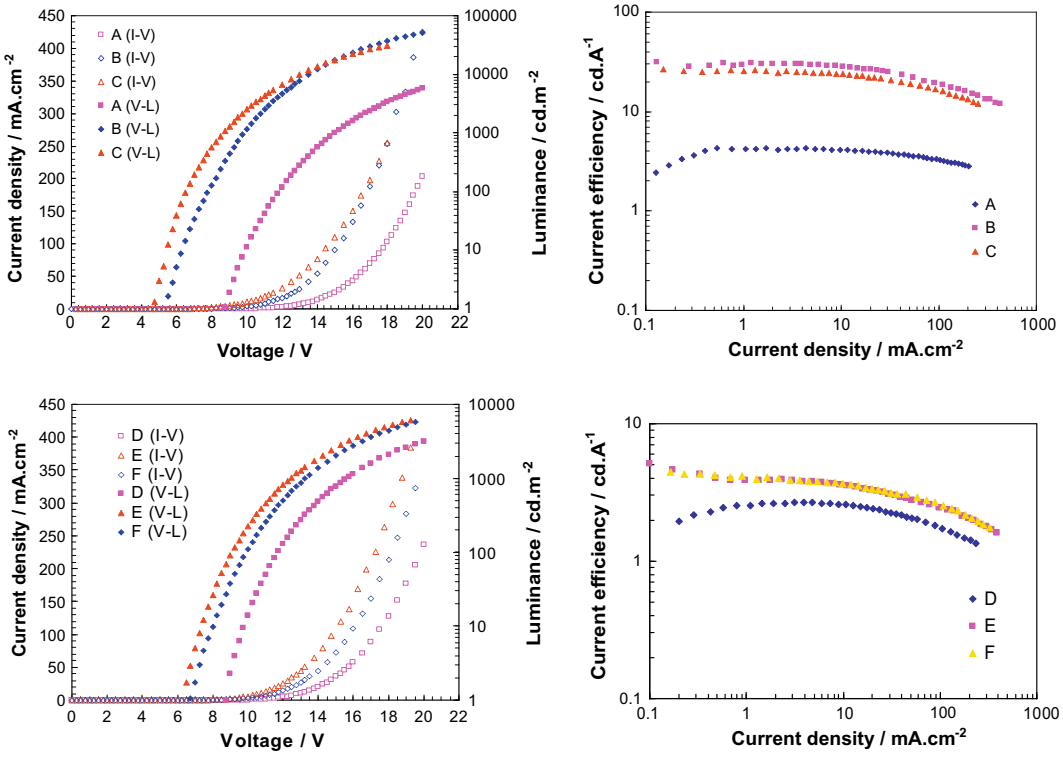

Fig. 4. Device performance of Complexes **A–C** (top) and Complexes **D–F** (bottom).

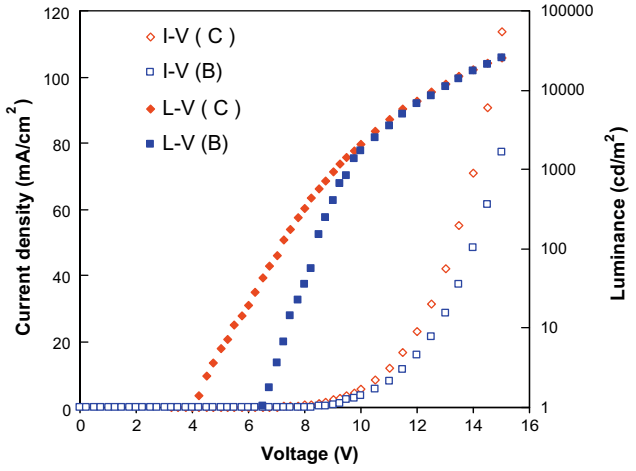

Fig. 6. Device performance of Complexes **B** and **C** with TPBI hole/exciton block layer.

enhanced. The maximum current efficiencies and external quantum efficiencies for Complexes **B** and **C** based devices are 46.3 cd/A (13.9%) and 42.5 cd/A (12.8%), respectively. In comparison to devices using BCP as the block layer, the efficiencies were increased by about 40%. The improvement of device performance should be ascribed to the better blocking effect of TPBI over BCP to holes/excitons.

4. Conclusion

In summary, a series of novel iridium-based organic phosphorescent materials with ligand bearing polyphenylphenyl dendron groups have been developed through simple synthesis and purification procedures. Good OLED device performance with tunable emission colors from yellow to saturated red has been demonstrated by doping the complex materials into PVK matrices. These solution processed OLED devices demonstrated quite stable EL efficiencies over a large range of current density, which indicated that the polyphenylphenyl dendron structure in the complexes could readily suppress the triplet–triplet annihilation.

References

[1] C.W. Tang, S.A. Van Slyke, Appl. Phys. Lett. 51 (1987) 913.
[2] J.H. Burroughes, D.D.C. Bradley, A.R. Brown, R.N. Marks, K. Mackay, R.H. Friend, P.L. Burn, A.B. Holmes, Nature (London) 347 (1990) 539.
[3] M.A. Baldo, D.F. O'Brien, Y. You, A. Shoustikov, S. Sibley, M.E. Thompson, S.R. Forrest, Nature (London) 395 (1998) 151.
[4] M.A. Baldo, M.E. Thompson, S.R. Forrest, Nature (London) 403 (2000) 750.
[5] M.K. Nazeeruddin, R. Humphry-Baker, D. Berner, S. Rivier, L. Zuppiroli, M. Graetzel, J. Am. Chem. Soc. 125 (2003) 8790.
[6] S. Lammansky, P. Djurovich, D. Murphy, F. Abdel-Razzaq, H.E. Lee, C. Adachi, P.E. Burrows, S.R. Forrest, M.E. Thompson, J. Am. Chem. Soc. 123 (2001) 4304.
[7] X. Gong, M.R. Robison, J.C. Ostrowski, D. Moses, G.C. Bazan, A.J. Heeger, Adv. Mater. 14 (2002) 581.
[8] X. Gong, J.C. Ostrowski, G.C. Bazan, D. Moses, A.J. Heeger, M.S. Liu, A.K.Y. Jen, Adv. Mater. 15 (2003) 45.
[9] C.Y. Jiang, W. Yang, J.B. Peng, S. Xiao, Y. Cao, Adv. Mater. 16 (2004) 537.
[10] L. Deng, P.T. Furuta, S. Garon, J. Li, D. Kavulak, M.E. Thompson, J.M. Frechet, J. Chem. Mater. 18 (2006) 386.
[11] B.M.J.S. Paulose, D.K. Rayabarapu, J.P. Duan, C.H. Cheng, Adv. Mater. 16 (2004) 2003.
[12] S. Tokito, M. Suzuki, F. Sato, M. Kamachi, K. Shirane, Org. Electron. 4 (2003) 105.
[13] Y. Hino, H. Kajii, Y. Ohmori, Org. Electron. 5 (2004) 265.
[14] H.C. Li, P.T. Chou, Y.H. Hu, Y.M. Cheng, R.S. Liu, Organometallics 24 (2005) 1329.
[15] T.H. Kwon, H.S. Cho, M.K. Kim, J.W. Kim, J.J. Kim, K.H. Lee, S.J. Park, I.S. Shin, H. Kim, D.M. Shin, Y.K. Chung, J.I. Hong, Organometallics 24 (2005) 1578.
[16] X.W. Zhang, J. Gao, C.L. Yang, L.N. Zhu, Z.G. Li, K. Zhang, J.G. Qin, H. You, G.G. Ma, Organomet. Chem. 691 (2006) 4312.
[17] L.Q. Chen, H. You, C.L. Yang, X.W. Zhang, J.G. Qin, D.G. Ma, J. Mater. Chem. 16 (2006) 3332.
[18] Q. Zhao, C.Y. Jiang, M. Shi, F.Y. Li, T. Yi, Y. Cao, C.H. Huang, Organometallics 25 (2006) 3631.
[19] H.Z. Xie, M.W. Liu, O.Y. Wang, X.H. Zhang, C.S. Lee, L.S. Hung, S.T. Lee, P.F. Teng, H.L. Kwong, H. Zheng, C.M. Che, Adv. Mater. 13 (2001) 1245.
[20] W.G. Zhu, C.Z. Liu, L.J. Su, W. Yang, M. Yuan, Y. Cao, J. Mater. Chem. 13 (2003) 50.
[21] X.-M. Yu, H.-S. Kwok, W.-Y. Wong, G.-J. Zhou, Chem. Mater. 18 (2006) 5097.
[22] T.D. Anthopoulos, M.J. Frampton, E.B. Namdas, P.L. Burn, I.D.W. Samuel, Adv. Mater. 16 (2004) 557.
[23] T.D. Anthopoulos, J.P.J. Markham, E.B. Namdas, J.R. Lawrence, I.D.W. Samuel, S.C. Lo, P.L. Burn, Org. Electron. 4 (2003) 71.
[24] M.J. Frampton, E.B. Namdas, S.C. Lo, P.L. Burn, I.D.W. Samuel, J. Mater. Chem. 14 (2004) 2881.
[25] S.C. Lo, E.B. Namdas, C.P. Shipley, J.P.J. Markham, T.D. Anthopolous, P.L. Burn, I.D.W. Samuel, Org. Electron. 7 (2006) 85.
[26] C.T. Chen, C.L. Chiang, Y.C. Lin, L.H. Chan, C.H. Huang, Z.W. Tsai, C.T. Chen, Org. Lett. 5 (2003) 1261.
[27] C. Huang, C.G. Zhen, S.P. Su, K.P. Loh, Z.K. Chen, Org. Lett. 7 (2005) 391.
[28] X.J. Xu, S.Y. Chen, G. Yu, C.A. Di, H. You, D.G. Ma, Y.Q. Liu, Adv. Mater. 19 (2007) 1281.
[29] S. Setayesh, A.C. Grimsdale, T. Weil, V. Enkelmann, K. Müllen, F. Meghdadi, E.J.W. List, G. Leising, J. Am. Chem. Soc. 123 (2001) 946.
[30] M. Velusamy, K.R.J. Thomas, C.H. Chen, J.T. Lin, Y.S. Wen, W.T. Hsieh, C.H. Lai, P.T. Chou, Dalton Trans. 18 (2007) 3025.
[31] N. Cumpstey, R.N. Bera, P.L. Burn, I.D.W. Samuel, Macromolecules 38 (2005) 9564.
[32] Z.K. Chen, C. Huang, C.G. Zhen, J.H. Yao, WO2006093466A1.
[33] H. Meng, Z.-K. Chen, W. Huang, J. Phys. Chem. B 103 (1999) 6429.
[34] Z.-K. Chen, W. Huang, L.-H. Wang, E.-T. Kang, B.-J. Chen, C.-S. Lee, S.-T. Lee, Macromolecules 33 (2000) 9015.
[35] G.F. He, S.C. Chang, F.C. Chen, Y.F. Li, Y. Tang, Appl. Phys. Lett. 81 (2002) 1509.
[36] J. Kalinowski, W. Stampor, J. Mezyk, M. Cocchi, D. Virgili, V. Fattori, P. Di Marco, Phys. Rev. B 66 (2002) 235321.
[37] Y. Kawamura, S. Yanagida, S.R. Forrest, J. Appl. Phys. 92 (2002) 87.
[38] X. Gong, J.C. Ostrowski, G.C. Bazan, D. Moses, A.J. Heeger, Appl. Phys. Lett. 81 (2002) 3711.